International Journal of Mechanical Engineering and Technology (IJMET)
Volume 8, Issue 3, March 2017, pp. 56–65 Article ID: IJMET_08_03_007
Available online at http://www.iaeme.com/IJMET/issues.asp?JType=IJMET&VType=8&IType=3
ISSN Print: 0976-6340 and ISSN Online: 0976-6359

COMPARISON OF RESPONSE TO UNBALANCE OF OVERHUNG ROTOR SYSTEM FOR DIFFERENT SUPPORTS

Rohit Tamrakar
PhD. Scholar, Department of Mechanical Engineering,
MANIT Bhopal, Madhya Pradesh, India

N.D. Mittal
Professor, Department of Mechanical Engineering,
MANIT Bhopal, Madhya Pradesh, India

ABSTRACT

Rotor unbalance is most common fault found in the rotating machines. Methods are adopted to analyze the position of unbalance and to bring its effect into acceptable limit. Vibration analysis is the most common technique used to analyze the rotor system. Research have been performed on rotor supported at both ends, however less study has been done for overhung rotor. In this paper the response of overhung rotor on isotropic support and anisotropic support subject to unbalance has been presented. Mathematical formulation is done using Finite Element method and equations are solved using MATLAB programming. The effect of unbalance has been studied on the bode plot. Forward and Reverse whirl are observed through Campbell diagram and mode shapes are plotted.

Key words: rotor, overhung, isotropic, anisotropic, Campbell, bode plot.

Cite this Article: Rohit Tamrakar and N.D. Mittal, Comparison of Response to Unbalance of Overhung Rotor System for Different Supports. *International Journal of Mechanical Engineering and Technology*, 8(3), 2017, pp. 56–65.
http://www.iaeme.com/IJMET/issues.asp?JType=IJMET&VType=8&IType=3

1. INTRODUCTION

The unbalance response of the rotor system is an important aspect to consider while designing a rotor. Finite Element Method (FEM) has proved out to be of great importance in study of the dynamics of rotor system especially for unbalance response due to its accuracy in the results [1, 2]. As the complexity of rotor problem increases the matrix size involved in the FEM analysis also increases and researches have been carried out for more than a decade to reduce the matrix size of the elements involves. Various Matrix reduction scheme have been proposed by researchers. Substructure synthesis method is one of the scheme which has gained importance which involves the division of the model into substructures followed by analyzing these substructures and finally compiling the results to give response of the overall

rotor system. An improved substructure synthesis method was presented for studying the unbalance response of multi-span rotor by introducing an exact matrix condensation scheme which reduces the size of the element matrix, consideration was made that a complicated rotor system consists mainly of multi-span rotors with less effect of coupling or bearings [3].

Model based identification techniques have been of keen interest of many researchers to study the dynamic behavior of the rotors. The most common technique for unbalance study is influence coefficient approach [4]. The response of rotors has been studied combining two or more defects. Hertzian contact force, surface waviness, internal radial clearance etc. are some of the non linearities which have been combined with unbalance effect to study the response of rotor. Response maps, Frequency maps, orbit plots and Poincare maps are used to analyze the output response of the rotor system [5-8]. Dynamic behavior of the rotor gets changed by the presence of faults like unbalance. The changes are due to change in the equivalent loads that arise from moments and forces due to the damage. The effects of these equivalent loads are studied by applying them on the undamaged model. The model with these loads mathematically is known as fault model. Fault models of rotor can be used to compare the effect of other defect like unbalance which can help to determine the position and phase of the unbalance [9]. The method of equivalent loads has a limitation that the number of measured vibrations has to be kept less to avoid errors. This is achieved through theoretical fault method and vibration minimization method. These methods can measure unbalance fault even for two degree of freedom cases and with less errors compared to equivalent loads method [10].

The misalignment at the coupling has been studied along with the unbalance effect to show the synchronous forces and moments exists which depends on the type and amount of misalignment between the rotors [11].

The study of overhung rotors has gained importance, since the overhung rotor has more effect of its deflection due to its weight on its dynamic analysis. The gravity has a softening effect on the analysis of overhung rotors bringing the system towards the linearity [12]**.**The sudden unbalance effect like sudden mass loss in turbines can cause an impact effect which can excite the rotor to its natural frequency. Bode plots have been successful to analyze any sudden change in the unbalance of the rotors [13].

2. MATHEMATICAL MODELING

The general equation of motion of overhung rotor system is given as:

$$M\ddot{q}+C\dot{q}+\Omega G\dot{q}+Kq=0 \quad \text{OR}$$

$$M\ddot{q}+(C+\Omega G)\dot{q}+Kq=0 \tag{1}$$

For calculation of Eigen values and Eigen vectors

$$\begin{bmatrix} C+\Omega G & M \\ M & 0 \end{bmatrix} \frac{d}{dt}\begin{Bmatrix} q \\ \dot{q} \end{Bmatrix} + \begin{bmatrix} K & 0 \\ 0 & -M \end{bmatrix} \begin{Bmatrix} q \\ \dot{q} \end{Bmatrix} = \begin{Bmatrix} 0 \\ 0 \end{Bmatrix} \tag{2}$$

$$A\dot{x}+Bx=0 \tag{3}$$

$$A=\begin{bmatrix} C+\Omega G & M \\ M & 0 \end{bmatrix} \quad B=\begin{bmatrix} K & 0 \\ 0 & -M \end{bmatrix} \quad x=\begin{Bmatrix} q \\ \dot{q} \end{Bmatrix} \tag{4}$$

where, M is the mass matrix, C is damping matrix, G is gyroscopic matrix, K is the stiffness matrix of the rotor system and q consists of the displacement and rotation terms at the nodes. The Gyroscopic forces and bearing properties varies with the shaft speed Ω, hence matrix A and B will also varies as the shaft speed vary. For Timoshenko beam element in which shear and rotary inertia effects are included Fig.1, the element has two degree of freedom at each node which makes the element consisting of four degree of freedom.

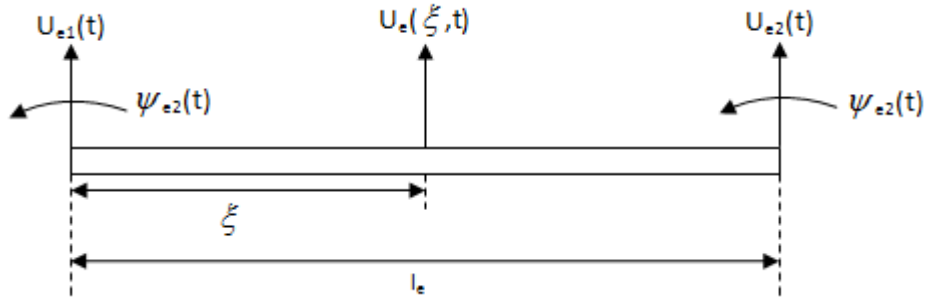

Figure 1 Local coordinates for beam element

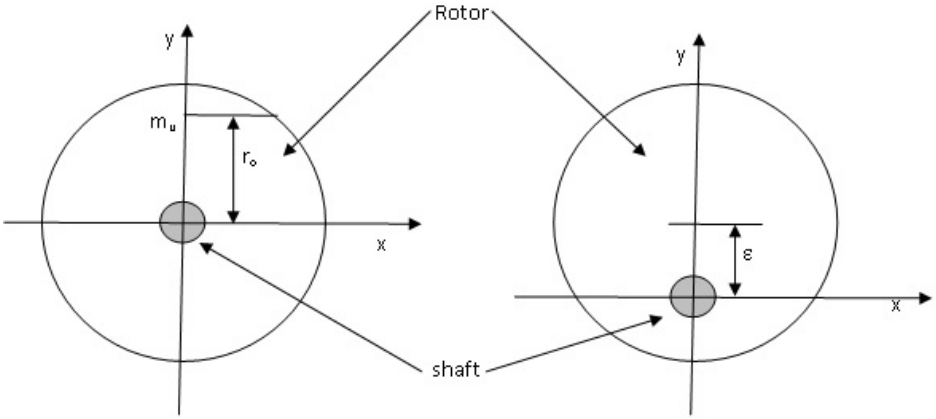

Figure 2 Model representing unbalance and eccentricity respectively

The unbalance response of the rotor system can be considered equal to the out of balance force response due to eccentricity. Hence for solving the unbalance response the forces generated due to eccentricity is considered for generation of equation of motion [14]**.**The eccentricity of the rotor is shown in Fig.2 which can be compared with the unbalance of m_u provided at the radius of r_o. The out of balance force due to eccentricity is $m\varepsilon\Omega^2$. The lateral acceleration of m_u is given as $m_u r_o\ \Omega^2$. If out of balance force due to eccentricity and mass unbalance are equal, then

$$m_u r_o = m\varepsilon \qquad (5)$$

where m is the total mass of the rotor and ε is the eccentricity, for equality to exist between the above models ε is small in comparison to r_o and m_u is small in comparison to m. Practically it is difficult to identify that whether the out of balance force exists due to eccentricity or mass unbalance. Study of unbalance is considered on Jeffcott rotor model with offset centre of mass from the shaft center line and the boundary conditions are applied for the overhung rotors.

The equations of Jeffcott rotor in Fig.3 for free vibration supported by isotropic bearing are given as [14]

$$
\begin{aligned}
&\mathrm{m}\,\ddot{x} + C_{xt}\,\dot{x} + C_{xc}\,\dot{y}_\theta + k_{xt}x + k_{xc}\,y_\theta = 0\\
&\mathrm{m}\,\ddot{y} + C_{yt}\,\dot{y} - C_{yc}\,\dot{x}_\theta + k_{yt}y - k_{yc}\,x_\theta = 0\\
&\mathrm{I}_d\,\ddot{x}_\theta + \mathrm{I}_p\Omega\,\dot{y}_\theta - C_{yc}\,\dot{y} + C_{yr}\,\dot{x}_\theta - k_{yc}\,y + k_{yr}\,x_\theta = 0\\
&\mathrm{I}_d\,\ddot{y}_\theta - \mathrm{I}_p\Omega\,\dot{x}_\theta + C_{xc}\,\dot{x} + C_{xr}\,\dot{y}_\theta + k_{xc}\,x + k_{xr}\,y_\theta = 0
\end{aligned}
\tag{6}
$$

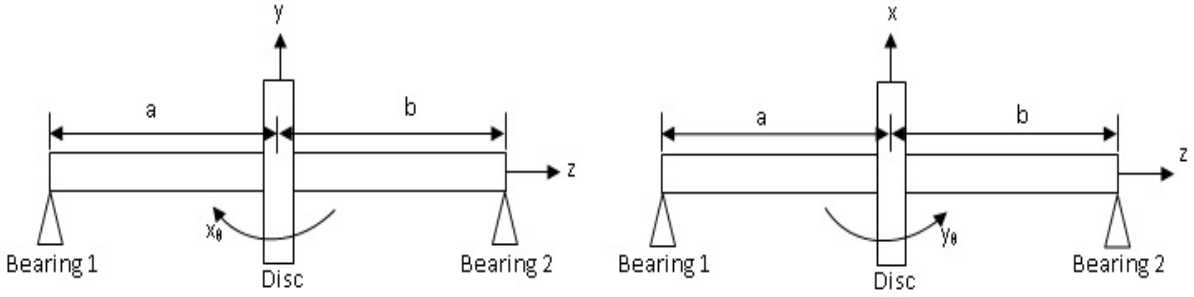

Figure 3 Jeffcott rotor view perpendicular to x-axis and y axis respectively

Where, x_θ and y_θ are displacement about x and y axis respectively. Due to the eccentricity ε the force is induced in these free vibration equations due to which there are changes in the dynamics behavior of the rotor system which are given in equation (7). The variable notation is provided in table 1.

$$
\begin{aligned}
&\mathrm{m}\,\ddot{u} + Ct\,\dot{u} + C_c\,\dot{y}_\theta + k_t u + k_c\,y_\theta = m\varepsilon\Omega^2\cos\Omega t\\
&\mathrm{m}\,\ddot{v} + C_t\,\dot{y} - C_c\,\dot{x}_\theta + k_t y - k_c\,x_\theta = m\varepsilon\Omega^2\sin\Omega t\\
&\mathrm{I}_d\,\ddot{x}_\theta + \mathrm{I}_p\Omega\,\dot{y}_\theta - C_c\,\dot{v} + C_r\,\dot{x}_\theta - k_c v + k_r\,x_\theta = 0\\
&\mathrm{I}_d\,\ddot{y}_\theta - \mathrm{I}_p\Omega\,\dot{x}_\theta + C_c\,\dot{u} + C_r\,\dot{y}_\theta + k_c\,u + k_r\,y_\theta = 0
\end{aligned}
\tag{7}
$$

Table 1 Variables used in equation (7)

Variable	Specification	Variable	Specification
k_{x1}	Stiffness of I bearing in x direction	c_{x2}	Damping of II bearing in x direction
k_{x2}	Stiffness of II bearing in x direction	c_{y1}	Damping of I bearing in y direction
k_{y1}	Stiffness of I bearing in y direction	c_{y2}	Damping of II bearing in y direction
k_{y2}	Stiffness of II bearing in y direction	C_{xt}	$c_{x1}+c_{x2}$
k_{yt}	$k_{x1}+k_{x2}$	C_{yt}	$c_{y1}+c_{y2}$
k_{xc}	$-ak_{x1}+bk_{x2}$	C_{xc}	$-ac_{x1}+bc_{x2}$
k_{xr}	$a^2k_{x1}+b^2k_{x2}$	C_{yc}	$-ac_{y1}+bc_{y2}$
k_{yc}	$-ak_{y1}+bk_{y2}$	C_{xr}	$a^2c_{x1}+b^2c_{x2}$
k_{yr}	$a^2k_{y1}+b^2k_{y2}$	C_{yr}	$a^2c_{y1}+b^2c_{y2}$
k_{yt}	$k_{y1}+k_{y2}$	I_d	Diametral moment of inertia of the disc
c_{x1}	Damping of I bearing in x direction	I_p	Polar moment of inertia of the rotor about z-axis

2.1. Unbalance Jeffcott Rotor Model Supported On Isotropic Bearings

For research purpose the rotor is assumed to be supported on isotropic bearing i.e. the stiffness of the bearing in the each direction is same, the equations (7) can be modified as

$$\begin{aligned}
&\mathrm{m}\ddot{u}+C_t\dot{u}+C_c\dot{y}_\theta+k_t u+k_c y_\theta = m\varepsilon\Omega^2\cos\Omega t\\
&\mathrm{m}\ddot{v}+C_t\dot{v}-C_c\dot{x}_\theta+k_t v-k_c x_\theta = m\varepsilon\Omega^2\sin\Omega t\\
&\mathrm{I}_d\ddot{x}_\theta+\mathrm{I}_p\Omega\dot{y}_\theta-C_c\dot{v}+C_r\dot{x}_\theta-k_c v+k_r x_\theta = 0\\
&\mathrm{I}_d\ddot{y}_\theta-\mathrm{I}_p\Omega\dot{x}_\theta+C_c\dot{u}+C_r\dot{y}_\theta+k_c u+k_r y_\theta = 0
\end{aligned} \tag{8}$$

where, $k_{xt}=k_{yt}=k_t$, $k_{xr}=k_{yr}=k_r$, $k_{xc}=k_{yc}=k_c$, $C_{xt}=C_{yt}=C_t$, $C_{xr}=C_{yr}=C_r$ $C_{xc}=C_{yc}=C_c$ for isotropic bearing. In matrix form of equation (1):

$$M=\begin{bmatrix} m & 0 & 0 & 0\\ 0 & m & 0 & 0\\ 0 & 0 & I_d & 0\\ 0 & 0 & 0 & I_d \end{bmatrix},\quad G=\begin{bmatrix} 0 & 0 & 0 & 0\\ 0 & 0 & 0 & 0\\ 0 & 0 & 0 & I_p\\ 0 & 0 & I_p & 0 \end{bmatrix},\quad C=\begin{bmatrix} C_t & 0 & 0 & C_c\\ 0 & C_t & -C_c & 0\\ 0 & -C_c & C_r & 0\\ C_c & 0 & 0 & C_r \end{bmatrix}$$

$$K=\begin{bmatrix} k_t & 0 & 0 & k_c\\ 0 & k_t & -k_c & 0\\ 0 & -k_c & k_r & 0\\ k_c & 0 & 0 & k_r \end{bmatrix},\quad q=\begin{bmatrix} u\\ v\\ \theta\\ \psi \end{bmatrix},\quad Q=\begin{bmatrix} m\varepsilon\Omega^2\cos\Omega t\\ m\varepsilon\Omega^2\sin\Omega t\\ 0\\ 0 \end{bmatrix} \tag{9}$$

2.2. Unbalance Jeffcott Rotor Model Supported On Anisotropic Bearings

Practically the bearings on which the rotor is supported have different stiffness in every plane. So it is necessary to analyze the response for anisotropic bearings. The matrices for equation (1) are given as:

$$M=\begin{bmatrix} m & 0 & 0 & 0\\ 0 & m & 0 & 0\\ 0 & 0 & I_d & 0\\ 0 & 0 & 0 & I_d \end{bmatrix},\quad G=\begin{bmatrix} 0 & 0 & 0 & 0\\ 0 & 0 & 0 & 0\\ 0 & 0 & 0 & I_p\\ 0 & 0 & I_p & 0 \end{bmatrix},\quad C=\begin{bmatrix} C_{xt} & 0 & 0 & C_{xc}\\ 0 & C_{yt} & -C_{cy} & 0\\ 0 & -C_{yc} & C_{yr} & 0\\ C_{xc} & 0 & 0 & C_{xr} \end{bmatrix}$$

$$K=\begin{bmatrix} k_{xt} & 0 & 0 & k_{xc}\\ 0 & k_{yt} & -k_{yc} & 0\\ 0 & -k_{yc} & k_{yr} & 0\\ k_{xc} & 0 & 0 & k_{xr} \end{bmatrix},\quad q=\begin{bmatrix} u\\ v\\ \theta\\ \psi \end{bmatrix},\quad Q=\begin{bmatrix} m\varepsilon\Omega^2\cos\Omega t\\ m\varepsilon\Omega^2\sin\Omega t\\ 0\\ 0 \end{bmatrix} \tag{10}$$

3. RESPONSE ANALYSIS AND RESULTS

The overhung rotor system has coupling between the displacements and rotations. Letting $r=u+jv$ and $\varphi=y_\theta-jx_\theta$ equation (8) can be combined to form a single pair of equations for isotropic support.

$$m\ddot{r}+c_t\dot{r}+c_c\dot{\varphi}+k_t r+k_c\varphi=m\varepsilon\Omega^2 e^{j\Omega t}$$

$$I_d\ddot{\varphi}-jI_p\Omega\dot{\varphi}+c_c\dot{r}+c_r\dot{\varphi}+k_c r+k_r\varphi=0 \quad (11)$$

The response of the system to out of balance force is given as [14]

$$r_o=\frac{m\varepsilon\Omega^2}{D}\left\{-(\mathrm{I_d}-\mathrm{I_p})\Omega^2+\mathrm{jc_r}\,\Omega+\mathrm{k_r}\right\} \quad (12)$$

$$\varphi_o=\frac{m\varepsilon\Omega^2}{D}\left\{-\mathrm{jc_c}\,\Omega-\mathrm{k_c}\right\} \quad (13)$$

Where, $D=(-(\mathrm{I_d}-\mathrm{I_p})\Omega^2+\mathrm{jc_r}\,\Omega+\mathrm{k_r})(-\mathrm{m}\Omega^2+\mathrm{jc_t}\,\Omega+\mathrm{k_t})-(\mathrm{jc_c}\,\Omega+\mathrm{k_c})^2$

Fig.4 shows the 3 dimensional view of the rotor system with two discs. The finite element modeling of the rotor-bearing-disc system has been done. This system is divided into 14 elements as shown in Fig. 5. Element size between bearings is kept 54.6 mm and after node 11 element size is 44.45 mm. The system carries two discs at node 6 and node 15. Shaft is supported by bearing at node 1 and node 11 representing an overhung rotor system. The unbalance mass m_u is attached to disc at node 15 at a distance of r_o from disc centre. Physical dimensions used for analysis are given in table 2. These parameters corresponds to the Machinery Fault system - Rotor Dynamics system (MFS-RDS) supplied by Spectra Quest. The material used for shaft is TGP steel and Aluminum for discs. For isotropic supports the value of k_x is used as bearing stiffness in both directions and for anisotropic supports k_x and k_y are used as bearing stiffness. The analysis is performed through MATLAB programming.

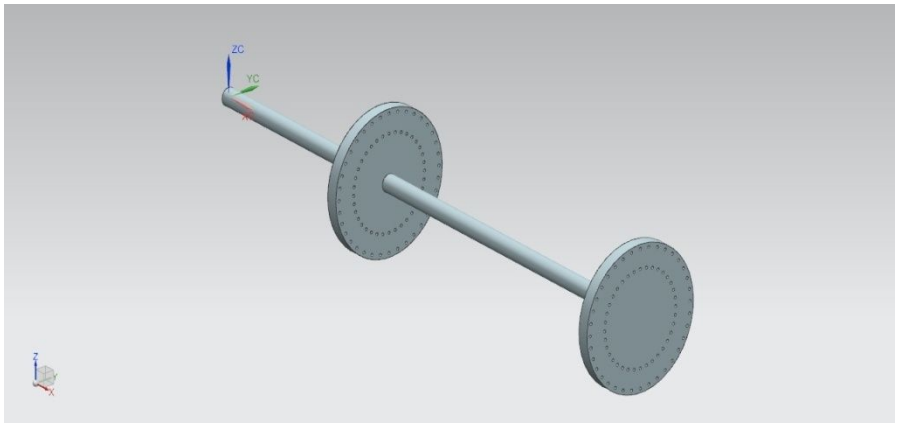

Figure 4 3-D model of the rotor system

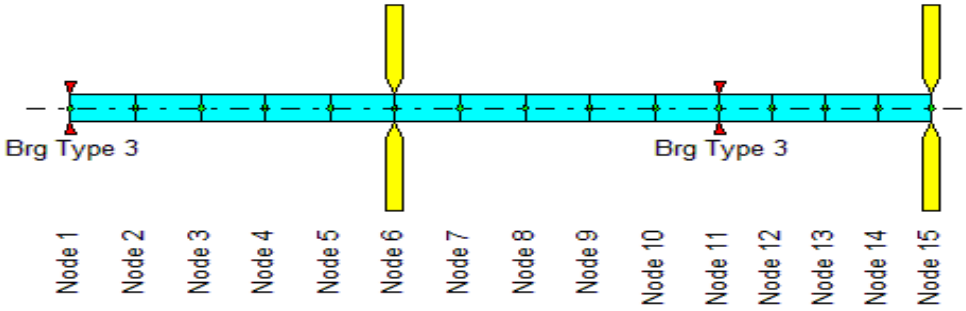

Figure 5 FEM modeling of rotor system

Table 2 Physical parameters of the rotor system

Parameter	Value	Parameter	Value
Total length of shaft	723.9 mm	k_x	7 x 10^7 N/m
Distance between bearings	546.1 mm	k_y	5 x 10^7 N/m
Diameter of discs	152.4 mm	$c_x = c_y$	5 x 10^2 Ns/m
Diameter of shaft	19.05 mm	m_u	5.43 gm
Disc thickness	14.27 mm	r_o	69.85 mm

3.1. Isotropic Support

Isotropic support has same stiffness in every direction. The response of unbalance is shown in Fig.7 through Bode plot diagram. In Fig.6 (a) we can see the response magnitude and phase change w.r.t. rotor spin speed for node 6 and node 15. The response of the unbalance which is provided at node 15 can be observed from the sudden fall in the response magnitude at 6860 rpm where the phase also gets changed by 180 degree which corresponds to the same response in [13]**.** The other two peaks of 3960 rpm and 8320 rpm show response for critical speed as seen from the Campbell diagram (Fig.7 a) and they are for forward whirl. The response in x and y direction at the same node for isotropic supports are always out of phase as seen from Fig.6 (b). The first four mode shapes for the rotor system supported on isotropic supports is shown in Fig. 7 (b), it can be seen that odd number modes are backward and even number modes are forward.

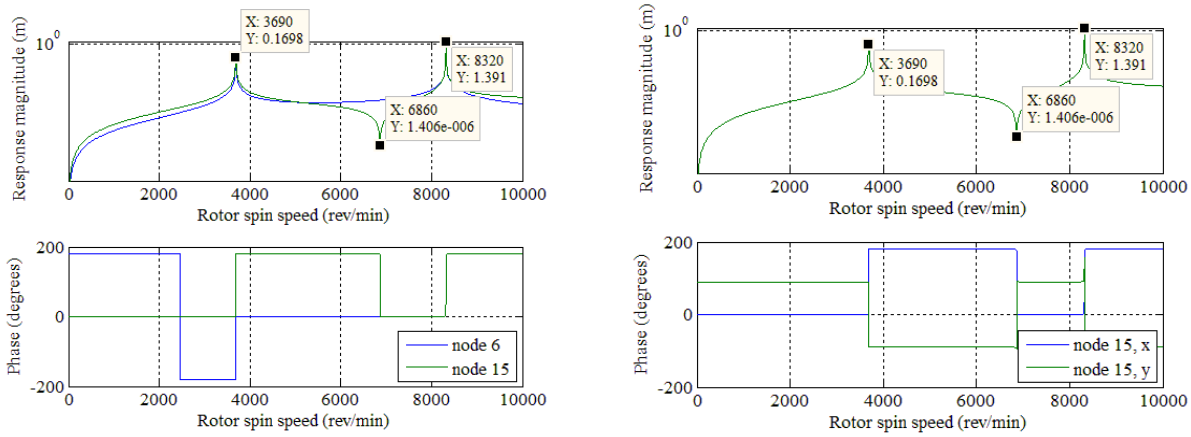

(a) Unbalance response for node 6 and 15 (b) unbalance response for node 15

Figure 6 Unbalance response for isotropic support

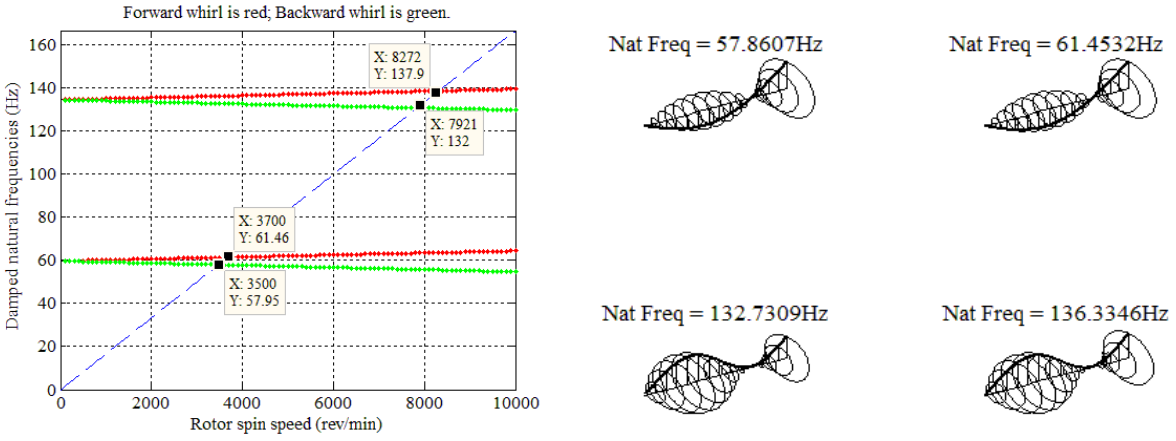

(a) Campbell Diagram (b) Mode shape

Figure 7 Campbell diagram and mode shape for isotropic support

3.2. Anisotropic Support

The response for anisotropic support is shown in Fig.8. The two peaks in response magnitude at 3690 rpm and 8310 Fig.8 (a) are of critical speed as seen from Campbell diagram in Fig.9 (a). There is sudden fall in response magnitude and change in phase at 6840 rpm which is due to unbalance response. There is some disturbance in response magnitude around 7830 rpm which can due to the mixed modes. The responses at 6840 rpm and 7830 rpm are of backward whirl which are shaded by yellow color in Fig.8 (b). The response for the same node in x and y direction is always out of phase as seen in Fig.8 (b). The odd number modes are backward and even number modes are forward as seen from Fig.9 (b).

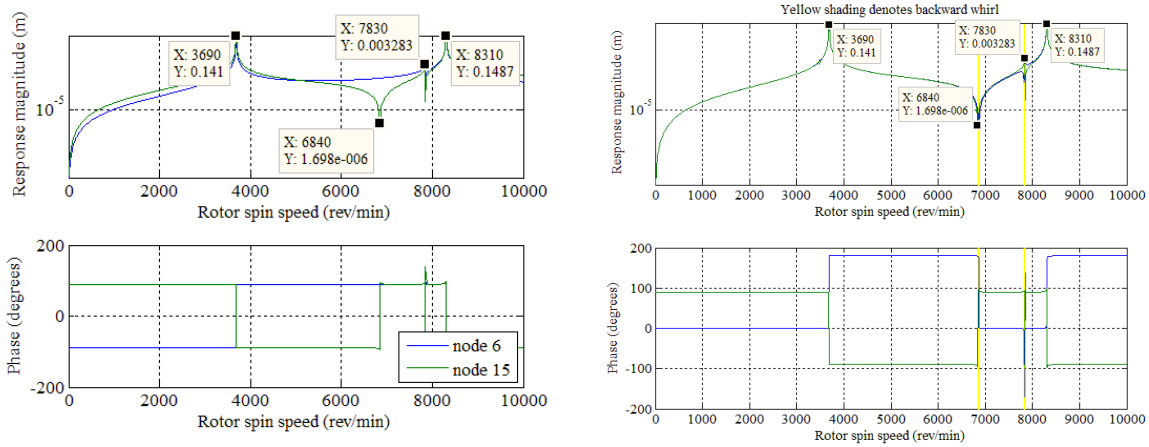

(a) Unbalance response for node 6 and 15 (b) Unbalance response for node 15 in x and y direction

Figure 8 Unbalance response for anisotropic support

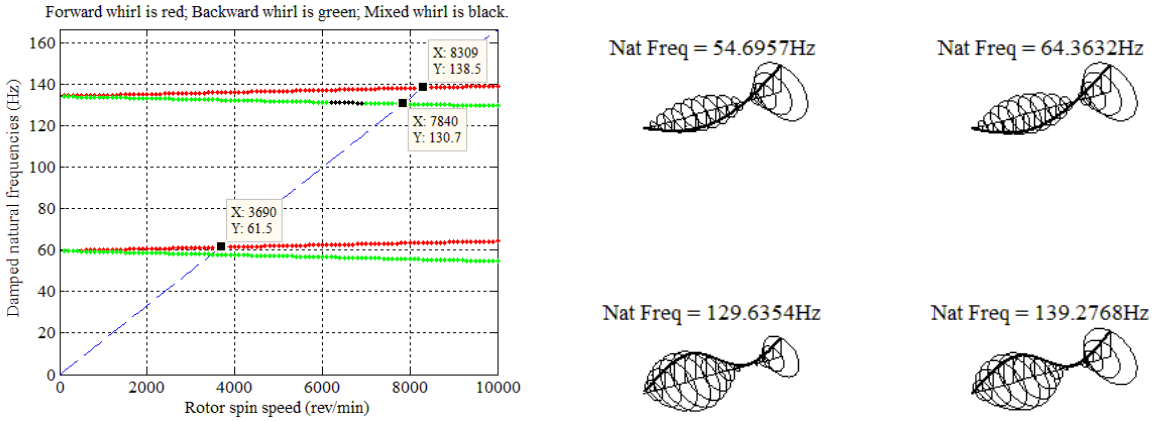

(a) Campbell diagram (b) Mode shape

Figure 9 Campbell Diagram and mode shape for anisotropic support

4. CONCLUSIONS

The response to unbalance of overhung rotor is studied on isotropic and anisotropic supports. The Bode plot is found to be useful in studying the unbalance response. There is sudden drop in the response magnitude due to unbalance for both the supports. Phase change is also seen where the amplitude suddenly drops due to unbalance in the rotor system. The response in anisotropic supports has mixed whirl for some range of rpm. The odd mode shapes are at slightly higher frequency for isotropic supports i.e. for backward whirl, where as the even modes shapes are at higher frequency for anisotropic supports i.e. for forward whirl.

REFERENCES

[1] Nelson, H.D., A Finite Rotating Shaft Element Using Timoshenko Beam Theory. Journal of Mechanical Design, 1980. 102(4): p. 793-793.

[2] Hashish, E. and T.S. Sankar, Finite Element and Modal Analyses of Rotor-Bearing Systems Under Stochastic Loading Conditions. Journal of Vibration Acoustics Stress and Reliability in Design, 1984. 106(1): p. 80-80.

[3] Hong, S.W. and J.H. Park, An efficient method for the unbalance response analysis of rotor-bearing systems. Journal of Sound and Vibration, 1997. 200(4): p. 491-504.

[4] Lees, A.W., J.K. Sinha, and M.I. Friswell, Model-based identification of rotating machines. Mechanical Systems and Signal Processing, 2009. 23(6): p. 1884-1893.

[5] Tiwari, M., K. Gupta, and O. Prakash, Dynamic Response of an Unbalanced Rotor Supported on Ball Bearings. Journal of Sound and Vibration, 2000. 238(5): p. 757-779.

[6] Harsha, S.P., K. Sandeep, and R. Prakash, The effect of speed of balanced rotor on nonlinear vibrations associated with ball bearings. International Journal of Mechanical Sciences, 2003. 45(4): p. 725-740.

[7] Yadav, H.K., S.H. Upadhyay, and S.P. Harsha, Study of effect of unbalanced forces for high speed rotor. Procedia Engineering, 2013. 64: p. 593-602.

[8] Harsha, S.P., Nonlinear dynamic response of a balanced rotor supported by rolling element bearings due to radial internal clearance effect. Mechanism and Machine Theory, 2006. 41(6): p. 688-706.

[9] Jain, J.R. and T.K. Kundra, Model based online diagnosis of unbalance and transverse fatigue crack in rotor systems. Mechanics Research Communications, 2004. 31(5): p. 557-568.

[10] Sudhakar, G.N.D.S. and A.S. Sekhar, Identification of unbalance in a rotor bearing system. Journal of Sound and Vibration, 2011. 330(10): p. 2299-2313.

[11] Sinha, J.K., A.W. Lees, and M.I. Friswell, Estimating unbalance and misalignment of a flexible rotating machine from a single run-down. Journal of Sound and Vibration, 2004. 272(3-5): p. 967-989.

[12] Tiaki, M.M., S.A.A. Hosseini, and M. Zamanian, Nonlinear forced vibrations analysis of overhung rotors with unbalanced disk. Archive of Applied Mechanics, 2016. 86(5): p. 797-817.

[13] Ma, Y., et al., BODE results - Experimental investigation on dynamical response of an overhung rotor. 2016.

[14] Friswell, M.I., et al., Dynamics of Rotating Machines. Cambridge: Cambridge University Press, 2010.

[15] M. Chandra Sekhar Reddy. Design and Analysis of Steam Turbine Rotor. *International Journal of Mechanical Engineering and Technology*, 6 (11), 2015, pp. 195-201.

[16] Abhishek Kr. Singh and Durg Vijay Rai, The Variation in Physical Properties Affects the Vertical Compressive Strength of The Rudraksha - Bead (Elaeocarpus Ganitrus Roxb). *International Journal of Mechanical Engineering and Technology*, 7(3), 2016, pp. 276–284.